[19] Dawson, L. G. and Holliday, J. B., "Propulsion, The Second Century Papers: Looking Ahead in Aeronautics—9," *The Aeronautical Journal of the Royal Aeronautical Society*, Vol. 72, No. 693, Sept. 1968, p. 739.

[20] Weir, R. H., "Propulsion Prospects," *The Aeronautical Journal of the Royal Aeronautical Society*, Vol. 73, No. 707, Nov. 1969, p. 923.

[21] "Transonic Aerodynamics," *NATO AGARD Conference Proceedings*, No. 35, Sept. 1968.

[22] Dachs, L. L., "Beryllium Disks Sop Up C-5A-Size Brake Heat Loads," *Space/Aeronautics*, Vol. 51, May 1969.

[23] "Nuclear Aircraft," Preliminary Design Proposal 74, April 1969, Lockheed-Georgia Co., Marietta, Ga.

[24] Rom, F. E., "Status of the Nuclear Powered Airplane," AIAA Paper 69-554, U.S. Air Force Academy, Colo., 1969.

NOV.-DEC. 1970 J. AIRCRAFT VOL. 7, NO. 6

Evaluation of the Design Parameters for Optimum Heavily Loaded Ducted Fans

TERRY WRIGHT*

Georgia Institute of Technology, Atlanta, Ga.

A consistent mathematical model for the ultimate vortex wake system of an optimum heavily loaded ducted fan has been developed for zero hub diameter and neglecting compressibility, viscosity, and tip clearance. The compatibility relationships to be satisfied are presented with a brief description of the model. For any choice of blade number and pitch angle, it is shown that the blade bound vortex strength distribution for the heavily loaded ducted fan may be extracted from the lightly loaded case through the use of a simple scaling factor. In addition, expressions are developed for the power, thrust, and induced efficiency for the heavily loaded system which may also be extracted from the lightly loaded results. Some sample results are presented for a ducted fan with 2, 4, 6, and 8 blades with loadings from a light load to the static thrust condition.

Nomenclature

b = number of blades
B_1 = defined as an integral, Eq. (16)
B_2 = defined as an integral, Eq. (17)
C_p = power coefficient, $C_p = P/\rho(\Omega R)^3\pi R^2$
C_T = thrust coefficient, $C_T = T/\rho(\Omega R)^2\pi R^2$
E = energy loss in the wake
e = nondimensional energy loss, $e = E/\rho(\Omega R)^3(\pi R^2)$
$f(t)$ = a function of time
G = scaling factor, Eq. (23)
$K(x)$ = nondimensional blade bound vortex strength distribution, Eq. (31)
L = characteristic axial length in wake, $L = 2\pi R\lambda/b$
$\bar{P}$ = nondimensional distance from a vortex element to a control point
p = static pressure
p_∞ = freestream static pressure
p_0 = total pressure
Q = torque
r,Ψ,z = cylindrical coordinates
r',Ψ',z' = cylindrical coordinates defining location of vortex filament
r,ξ,ζ = helical coordinates
R = blade tip radius, wake radius
S = surface area
dS = elemental surface area
T = total thrust of ducted fan
t = time
u = disturbance velocity in direction of subscript
u_{vs} = induced velocity, at $\bar{w} = 0$, associated with the inner helical sheets and the nonuniform boundary sheet
u_{ξ_0} = disturbance velocity component along wake axis
u_R = disturbance velocity component at inside of wake boundary
u_{ζ_B} = velocity component normal to filaments of the uniform boundary sheet
v = total disturbance velocity
V = velocity in ultimate wake
V_R = velocity at inside of wake boundary
V_∞ = axial flight velocity
w = apparent axial displacement velocity of blade trailing vortex sheets
$\bar{w}$ = nondimensional displacement velocity, $\bar{w} = w/\Omega R$
x,y,z = cartesian coordinates
x = nondimensional blade radial station, $x = r/R$
z_0' = distance between the $z = 0$ plane and the point where the filament intersects the xz plane
β = angle between the normals to the vectors $d\bar{s}'$ and $\bar{P}$ measured in the plane determined by $d\bar{s}$ and $\bar{P}$
$\Gamma(x)$ = blade bound vortex strength distribution
γ = a vortex filament strength
$\gamma(\zeta_B)$ = strength of boundary sheet at its lines of intersection with inner sheets
γ_i = vortex filament strength of finite unknown strength filaments replacing sheets of wake
$\bar{\gamma}_i$ = nondimensional filament strength, Eq. (27) $\bar{\gamma}_i = \gamma_i/(4\pi RwG)$
ϵ_0 = numerically integrated factor for $\bar{w} = 0$, Eq. (39)
κ = mass coefficient, $\kappa = 2\int_0^1 K(x)\,xdx$
λ = tangent of helix pitch angle of inner sheets $(V_\infty + w)/\Omega R$
λ_B = tangent of helix pitch angle of boundary filaments at their lines of intersection with inner sheets $(V_\infty + w_B)/\Omega R$
ρ = fluid density

Received October 13, 1969; revision received February 6, 1970. This work was supported by the U.S. Army Research Office, Durham, N.C., under Contract DAHC04 68 C 004 as a part of the doctoral thesis of the author under the direction of R. B. Gray.

* Senior Engineer, Fluid Systems Laboratory, Westinghouse Electric Corporation, West Lafayette, Ind.

φ = pitch angle of inner sheet filaments
φ_B = pitch angle of boundary filaments at their lines of intersection with inner sheets
φ_{rB} = dummy pitch angle related to φ_B
φ_R = pitch angle of outermost filament of inner sheet
Φ = disturbance velocity potential
Ω = blade rotational velocity
η_i = ideal or induced efficiency, Eq. (43)

Introduction

FOR the optimum ducted fan in axial flight the considerations of Betz[1] hold concerning the geometry and motion of the helical vortex sheets of the ultimate wake that are shed from the blade trailing edges. That is, the geometric pitch of each filament of these sheets must be constant and the sheets must appear to move as rigid screw surfaces. In addition it is necessary that the Kutta condition be satisfied at the duct trailing edge. Thus a sheet of vorticity must be shed from the duct trailing edge forming a boundary sheet of vortex filaments enclosing the screw-like sheets shed from the blades. For the heavily loaded system the inner vortex sheet must have an axial motion different from that of the boundary sheet. The description of this motion and the development of the necessary compatibility relationships were presented in some detail by Gray and Wright[2] and are summarized with the essential results below. In both this analysis and the analysis of Ref. 2, the effects of hub diameter, compressibility, viscosity, and tip clearance are neglected.

The principal difference between the arguments for the heavily loaded and lightly loaded cases is that, for the heavily loaded ducted fan, the disturbance velocity in the ultimate wake is not normal to the inner vortex sheet surfaces. More information about this difference is obtained through a consideration of the flowfields associated with the vortex systems. It was shown in Ref. 2 that, in order to limit the disturbance velocities to the inside of the wake and to assure irrotationality outside of the wake, the vortex strength and motion of the cylindrical boundary sheet must be governed by

$$u_{\zeta_B} = (\tfrac{1}{2})(u_{\xi_0}{}^2 \sin^2\varphi_R + w^2 \cos^2\varphi_R)^{1/2}$$

and

$$\gamma(\zeta_B) = (u_{\xi_0}{}^2 \sin^2\varphi_R + w^2 \cos^2\varphi_R)^{1/2}$$

where

$$u_{\xi_0} = w/\lambda[(\lambda - \lambda_B)/(1 + \lambda\lambda_B)] \tag{1}$$

The coordinates ζ and ξ are illustrated in Fig. 1. These two relationships are obtained directly from the conditions that the disturbance velocities are zero outside the wake, that the strength of a vortex sheet is equal to the discontinuity in the velocity components as the sheet is crossed, and that the motion of the sheet along the line of discontinuity is equal to the mean value of the velocity on either side. Thus, when relative motion exists between the inner sheets and the boundary filaments, that is for a heavily loaded system, the two vortex systems are related through the equations for $u_{\delta\beta}$ and $\gamma(\zeta_B)$, but only along the lines of intersection of the inner sheets and the cylindrical boundary. On the wake boundary between these helical lines of intersection, the filament density or sheet strength and the filament pitch angle must vary with the helical coordinate ζ.

In order to avoid having to solve for both the strength and the geometry of the boundary vortex sheet, this sheet is replaced by two simpler sheets whose combined effects satisfy the constraints placed upon a single boundary sheet. The first sheet has constant strength $\gamma(\zeta_B)$ and constant filament pitch angle φ_B and satisfies the compatibility conditions at the intersection lines. The second sheet has a varying strength and constant filament pitch angle φ_R and satisfies the radial velocity constraints. The subsequent superposition of these sheets must maintain the apparent rigid motion of the inner screw surfaces. The function and behavior of these sheets are discussed in more detail in Ref. 2.

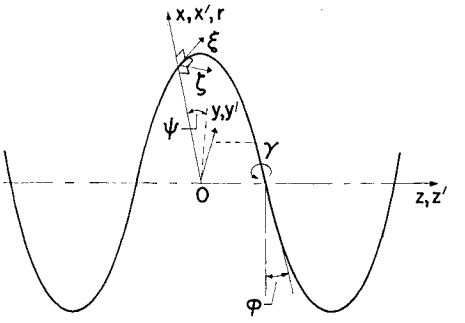

Fig. 1 Helical coordinate system.

On the basis of the compatibility conditions it can be shown that

$$\lambda_B = \lambda - \frac{\lambda^2 + 1}{2\lambda - \bar{w}} + \left[\left(\lambda - \frac{\lambda^2 + 1}{2\lambda - \bar{w}}\right)^2 + 1\right]^{1/2} \tag{2}$$

and

$$\gamma(\zeta_B) = w \cos\varphi_R \sec(\varphi_R - \varphi_B) \tag{3}$$

where $\varphi_B = \tan^{-1}(\lambda_B)$, and $\bar{w} = w/\Omega R$, $0 \leq \bar{w} \leq \lambda$.

The ultimate wake vortex system of the heavily loaded ducted fan is thus defined in terms of the inner helical sheets, a boundary sheet of uniform strength and pitch angle φ_B, and a boundary sheet of varying strength but constant pitch angle φ_R. The solution for the strength of the variable strength boundary sheet, for the strength distribution of the inner helical sheets, and thus for the blade bound vortex strength distribution, proceeds directly from the numerical integration of the Biot-Savart equation for the velocity at certain control points that is associated with each vortex filament in the wake model.

Analysis

The problem consists of two parts: first, the optimum blade bound vortex strength distribution must be determined in terms of the parameters λ, b, and $\bar{w}$; and second, the thrust, power, and induced efficiency of this optimum ducted fan must be determined. Both parts of the problem may be solved by finding the distribution of vorticity in the ultimate wake which will satisfy the boundary conditions implied by the geometry and motion specified in terms of λ, b, and $\bar{w}$.

Blade Bound Vortex Strength Distribution

In this analysis the Biot-Savart equation supplies the required relationship between the geometry, motion, and vortex strength in the ultimate wake. The vortex sheets of the system are divided into strips along the filament directions and these strips are replaced by finite strength vortex filaments equal in strength to the integrated sheet strength across the strip. The integrated velocity associated with one of these filaments, in terms of helical velocity components becomes

$$\frac{\Delta u_r}{w} = \frac{\gamma}{4\pi R w}\int_{-\infty}^{\infty}\left\{\bar{r}'\tan\varphi_R \sin(\Psi' - \Psi) + \bar{r}'(\bar{z} - \bar{z}_0' - \Psi'\tan\varphi_R)\cos(\Psi' - \Psi)\right\}\frac{d\Psi'}{\bar{P}^3} \tag{4}$$

$$\frac{\Delta u_\xi}{w} = \frac{\gamma\cos\varphi}{4\pi R w}\int_{-\infty}^{\infty}\left\{\bar{r}'\tan\varphi_R\left[\frac{\bar{r}}{\bar{r}'} + \frac{\bar{r}}{\bar{r}'} - 2\cos(\Psi' - \Psi)\right] + (\bar{z} - \bar{z}_0' - \Psi'\tan\varphi_R)\sin(\Psi' - \Psi)\right\}\frac{d\Psi'}{\bar{P}^3} \tag{5}$$

$$\frac{\Delta u_\varphi}{w} = \frac{\gamma \cos\varphi}{4\pi R w} \int_{-\infty}^{\infty} \left\{ \bar{r}'^2 - \bar{r}\bar{r}' \cos(\Psi' - \Psi) - \tan^2\varphi_R \left[1 - \frac{\bar{r}'}{\bar{r}} \cos(\Psi' - \Psi) \right] - \frac{\bar{r}'}{\bar{r}} \sin(\Psi' - \Psi) \times \tan\varphi_R (\bar{z} - \bar{z}_0' - \Psi' \tan\varphi_R) \right\} \frac{d\Psi'}{\bar{P}^3} \quad (6)$$

where

$$\bar{P}^2 = \bar{r}^2 + \bar{r}'^2 - 2\bar{r}\bar{r}' \cos(\Psi' - \Psi) + (\bar{z} - \bar{z}_0' - \Psi' \tan\varphi_R)^2$$

$$\varphi = \tan^{-1}$$

and $\bar{r}$, $\bar{r}'$, $\bar{z}$, $\bar{z}_0'$ are nondimensionalized by R.

$$[(1/\bar{r}) \tan\varphi_R]$$

The boundary conditions to be satisfied by the system at control points on the inner sheets and on the cylindrical boundary are as follows:

on the inner sheet

$$\sum(\Delta u_\xi/w) = \cos\varphi \quad (7)$$

$$\sum(\Delta u_r/w) = 0 \quad (8)$$

on the cylindrical boundary

$$\sum(\Delta u_r/w) = 0 \quad (9)$$

An additional constraint, necessary to insure a unique solution, is that the sum of the strengths of all of the vortex filaments comprising the system be zero. Considerations of symmetry enable the system of equations to be reduced to the following form:

on the inner sheet

$$\sum_1\left(\frac{\Delta u_\xi}{w}\right) + \sum_2\left(\frac{\Delta u_\xi}{w}\right) \cos(\varphi - \varphi_{rB}) - \sum_2\left(\frac{\Delta u_\xi}{w}\right) \sin(\varphi - \varphi_{rB}) + \sum_3\left(\frac{\Delta u_\xi}{w}\right) = \cos\varphi \quad (10)$$

on the cylindrical boundary

$$\Sigma_1(\Delta u_r/w) + \Sigma_3(\Delta u_r/w) = 0 \quad (11)$$

and

$$\Sigma_1(\gamma) + \Sigma_2(\gamma) + \Sigma_3(\gamma) = 0 \quad (12)$$

where Σ_1 is over the filaments of the inner sheets, Σ_2 is over the filaments of the uniform boundary sheet, and Σ_3 is over the filaments of the nonuniform boundary sheet;

$$\tan\varphi = (1/\bar{r}) \tan\varphi_R, \text{ and } \tan\varphi_{rB} = (1/\bar{r}) \tan\varphi_B$$

For a fixed choice of λ and $\bar{w}$, the contributions of the uniform boundary sheet to these equations are fixed in terms of the sheet strength $\gamma(\zeta_B)$ and the pitch angle φ_B, so that the system of equations can be rewritten as

$$\Sigma_1\left(\frac{\Delta u_\xi}{w}\right) + \Sigma_3\left(\frac{\Delta u_\xi}{w}\right) = \cos\varphi - \left[\Sigma_2\left(\frac{\Delta u_\xi}{w}\right) \times \cos(\varphi - \varphi_{rB}) - \Sigma_2\left(\frac{\Delta u_\xi}{w}\right) \sin(\varphi - \varphi_{rB}) \right] \quad (13)$$

$$\Sigma_1(\Delta u_r/w) + \Sigma_3(\Delta u_r/w) = 0 \quad (14)$$

$$\Sigma_1(\gamma) + \Sigma_3(\gamma) = -\Sigma_2(\gamma) \quad (15)$$

The integrals of the velocity components [Eqs. (4) and (6)] may be defined by

$$B_1 = (\Delta u_\xi/w)/[(\gamma/4\pi R w) \cos\varphi] \quad (16)$$

$$B_2 = (\Delta u_r/w)/(\gamma/4\pi R w) \quad (17)$$

Then, numbering γ_i over the filaments of the inner sheet and the nonuniform boundary sheet, the equations become the following:

for the control points on the inner sheet

$$\Sigma_i\left(\frac{\gamma_i}{4\pi R w}\right) B_{1i} = 1 - \left[\left\{ \Sigma_2\left(\frac{\Delta u_\xi}{w}\right) \cos(\varphi - \varphi_{rB}) - \Sigma_2\left(\frac{\Delta u_\xi}{w}\right) \sin(\varphi - \varphi_{rB}) \right\} / \cos\varphi \right] \quad (18)$$

for the control points on the cylindrical boundary

$$\Sigma_i(\gamma_i/4\pi R w) B_{2i} = 0 \quad (19)$$

and

$$\Sigma_i(\gamma_i/4\pi R w) = -\Sigma_2(\gamma/4\pi R w) \quad (20)$$

In this form the influence of $\bar{w}$ is confined to the right hand sides of the equations through the influence of the uniform boundary sheet. That is, the coefficients, B_{1i} and B_{2i}, of the unknowns, γ_i, depend only on the choice of λ and b.

Owing to the simplicity of the uniform boundary sheet, the integrands for the velocity field inside the wake associated with this sheet can be set up and evaluated explicitly in terms of λ and $\bar{w}$. The result of the integration is given as; $u_z/w = [\gamma(\zeta_B)/w] \cos\varphi_B$, $u_\Psi/w = 0$, $u_r/w = 0$.

u_z/w can be written from Eq. (3) as $u_z/w = \cos\varphi_R \sec(\varphi_R - \varphi_B) \cos\varphi_B$ or $u_z/w = 1/(1 + \lambda\lambda_B)$. Then

$$1 - \{ [\Sigma_2 (\Delta u_\xi/w) \cos(\varphi - \varphi_{rB}) - \Sigma_2(\Delta u_\xi/w) \times \sin(\varphi - \varphi_{rB})]/\cos\varphi \} = 1 - 1/1 + \lambda\lambda_B \quad (21)$$

Further

$$\Sigma_2(\gamma/4\pi R w) = [\gamma(\zeta_B)/4\pi R w](2\pi R \lambda_B \cos\varphi_{B/b})$$

where $2\pi R\lambda_B \cos\varphi_{B/b}$ is the characteristic sheet length normal to the filaments. Thus,

$$\Sigma_2(\gamma/4\pi R w) = 1/2b \cdot \lambda_B/(1 + \lambda\lambda_B) \quad (22)$$

Rearranging these terms

$$1 - 1/(1 + \lambda\lambda_B) = \lambda^2/(1 + \lambda^2) \times \{1 - (1/\lambda)[(\lambda - \lambda_B)/(1 + \lambda\lambda_B)]\}$$

and

$$[1/2b]\lambda_B/(1 + \lambda\lambda_B) = (1/2b)[\lambda/(1 + \lambda^2)] \times \{1 - (1/\lambda)[(\lambda - \lambda_B)/(1 + \lambda\lambda_B)]\}$$

But, from Eq. (1)

$$\bar{u}_{\xi_0} = (1/\lambda)[(\lambda - \lambda_B)/(1 + \lambda\lambda_B)]$$

so that, upon defining

$$G = 1 - \bar{u}_{\xi_0} \quad (23)$$

then

$$1 - [1/(1 + \lambda\lambda_B)] = G[\lambda^2/(1 + \lambda^2)]$$

and

$$(1/2b)[\lambda_B/(1 + \lambda\lambda_B)] = G[\lambda/(1 + \lambda^2)](1/2b)$$

The system of Eqs. (19–21) can then be written as

$$\Sigma_i(\gamma_i/4\pi R w) B_{1i} = G[(\lambda^2/(1 + \lambda^2)] \quad (24)$$

$$\Sigma_i(\gamma_i/4\pi R w) B_{2i} = 0 \quad (25)$$

$$\Sigma_i(\gamma_i/4\pi R w) = -G[\lambda/(1 + \lambda^2)](1/2b) \quad (26)$$

Then, defining

$$\bar{\gamma}_i = (\gamma_i/4\pi R w)/G \quad (27)$$

the sytem becomes

for control points on the inner sheet

$$\Sigma_i \bar{\gamma}_i B_{1i} = \lambda^2/(1 + \lambda^2) \tag{28}$$

for control points on the cylindrical boundary

$$\Sigma_i \bar{\gamma}_i B_{2i} = 0 \tag{29}$$

and

$$\Sigma_i \bar{\gamma}_i = -(1/2b)[\lambda/(1 + \lambda^2)] \tag{30}$$

Thus, for a fixed choice of λ and b, the system is solved with $G = 1$ ($\bar{w} = 0$) and the wake vorticity distribution for any value of $\bar{w}$ is obtained by multiplying the result by the appropriate value of G. The nondimensional blade bound vortex strength distribution $K(x)$ is defined as

$$K(x) = b\Gamma(x)/2\pi Rw\lambda \tag{31}$$

and is calculated by summing the filaments of an inner helical sheet lying inboard of the wake radius corresponding to the blade radial station, x, to yield $\Gamma(x)$. The remaining elements of the solution, the strengths of the filaments of the nonuniform boundary sheet, are required in the calculation of the thrust and power.

Thrust, Power, and Efficiency

Considering the control volume shown in Fig. 2 and using the momentum theorem, the thrust of the heavily loaded ducted fan is found by calculating the average pressure forces acting on the control surfaces and the average time rate of change of momentum of the fluid within the control volume. Averages are taken over a time $\Delta t = 2\pi/b\Omega$ and integration is with respect to time $dt = dz/(v_\infty + w)$. Following the analysis of Theodorsen[3] the thrust can be written as

$$T + \frac{1}{\Delta t}\int_{S_1,S_2} pdtdS = \frac{1}{\Delta t}\int_{S_2} \rho(V_\infty + u_z)\, dt(V_\infty + w)dS - \frac{1}{\Delta t}\int_{S_1} \rho V_\infty dt V_\infty dS$$

The pressure term can be eliminated through use of the z-component of Euler's equation

$$(\partial\Phi/\partial t) + (p/\rho) + \tfrac{1}{2}V^2 + f(t) = (p_\infty/\rho) + \tfrac{1}{2}V_\infty^2 = p_0/\rho$$

The unsteady term may be eliminated by considering the potential field in a steady coordinate system such that $\Phi(z, r, \Psi) = \Phi(z, r, \psi_0 + \Omega rt)$. Then

$$\partial\Phi/\partial t = (\partial\Phi/\partial\Psi)(\partial\Psi/\partial t) = u_\psi \Omega r = -(V_\infty + w)u_z + w(V_\infty + w)(1 - G)$$

Then $p/\rho + V^2/2 - (V_\infty + w)[u_z - w(1 - G)] = p_0/\rho$. At the cylindrical wake boundary the static pressure inside must equal the static pressure outside. Since there are no disturbance velocities outside the wake

$$(p_\infty - p) = (\rho/2)(V^2 - V_R^2) + \rho(V_\infty + w)(u_{zR} - u_z) \tag{32}$$

where

$$V^2 = (V_\infty + u_z)^2 + u_r^2 + u_\psi^2,\quad V_R^2 = (V_\infty + u_{zR})^2 + u_{\psi R}^2$$

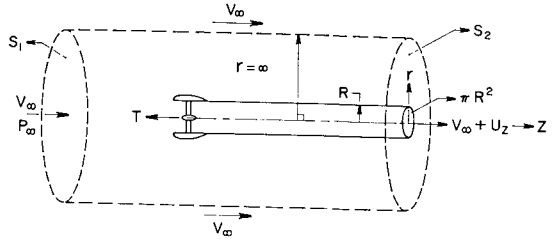

Fig. 2 Control volume for determining the thrust.

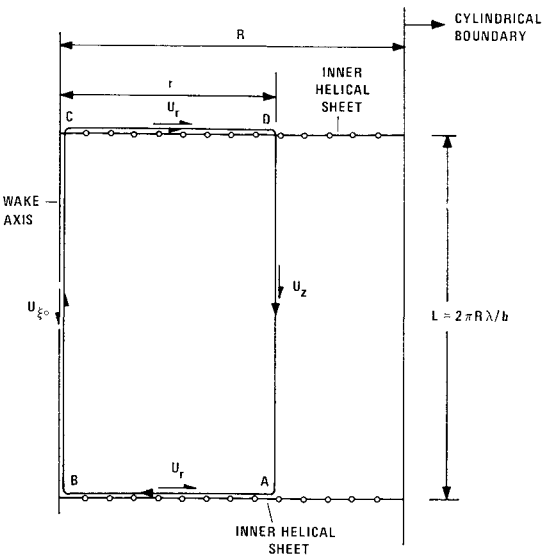

Fig. 3 Path of line integration in wake.

Substituting these values into Eq. (32) and simplifying the result yields

$$T = \frac{b\Omega\rho}{2\pi(V_\infty + w)}\int_{\substack{\text{characteristic}\\ \text{wake volume}}} \Big[V_\infty u_z + u_z^2 - \frac{1}{2}[(V_\infty + u_z)^2 - (V_\infty + u_{zR})^2 + u_r^2 + u_\Psi^2 - u_{\Psi R}^2] + (V_\infty + w)(u_z - u_{zR})\Big] dzdS \tag{33}$$

Now, nondimensionalizing the lengths as $\bar{z} = z/(2\pi R\lambda/b)$, $\bar{r} = r/R$, nondimensionalizing the disturbance velocities by w, and defining a thrust coefficient as $C_T = T/(\rho(\Omega R)^2\pi R^2)$ yields

$$C_T = 2\bar{w}^2\int_0^1\int_0^1\int_0^{2\pi}\Big[\frac{\lambda}{\bar{w}}\bar{u}_z + \frac{1}{2}\bar{u}_z^2 - \frac{1}{2}(\bar{u}_r^2 + \bar{u}_\psi^2) + \frac{1}{2}(\bar{u}_{zR}^2 + \bar{u}_{\Psi R}^2) - \bar{u}_{zR}\Big]\frac{\bar{r}d\bar{r}d\bar{z}d\Psi}{2\pi} \tag{34}$$

The $\bar{u}_z$ and $\bar{u}_{zR}$ terms can be eliminated from the integration through consideration of the line integral of velocity as shown in Fig. 3. The integral about the path ABCDA encloses those filaments shed by a blade bound vortex between $\bar{r} = 0$ and $\bar{r} = \bar{r}$ so that the line integral is equal to $\Gamma(\bar{r})$, or

$$\int_A^B u_r dr + \int_B^C u_z dz + \int_C^D u_r dr + \int_D^A u_z d_z = \Gamma(\bar{r})$$

But

$$\int_A^B u_r dr = -\int_C^D u_r dr \text{ and } \int_B^C u_z dz = -u_{\xi_0}L$$

so that

$$\int_D^A u_z dz = \Gamma(\bar{r}) + u_{\xi_0}L \tag{35}$$

Then

$$\int_0^1\int_0^1\int_0^{2\pi}\frac{\bar{u}_z d\bar{z}\bar{r}d\bar{r}d\Psi}{2\pi} = \int_0^1 K(\bar{r})\bar{r}dr + \bar{u}_{\xi_0}\int_0^1 \bar{r}d\bar{r}$$

and, following the definition of Theodorsen[3]

$$\kappa = 2\int_0^1 K(x)xdx \tag{36}$$

Thus,

$$\int_0^1\int_0^1\int_0^{2\pi}\frac{\bar{u}_z d\bar{z}\bar{r}d\bar{r}d\Psi}{2\pi} = \frac{1}{2}(\kappa + \bar{u}_{\xi 0}) \tag{37}$$

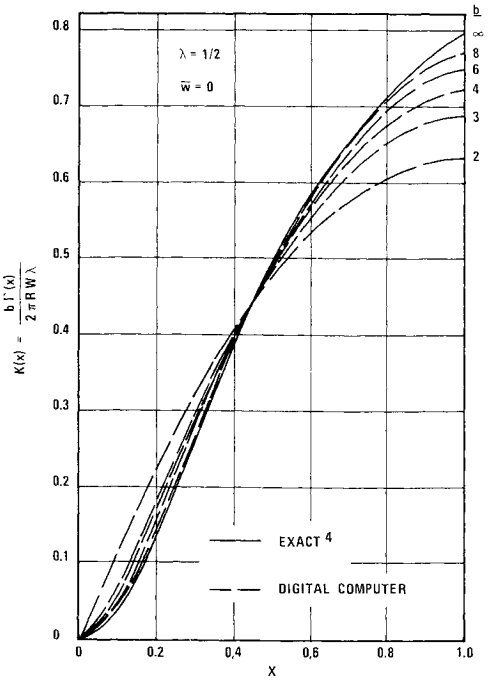

Fig. 4 Blade bound circulation distribution.

Similarly

$$\int_0^1\int_0^1\int_0^{2\pi} \frac{\bar{u}_{z_R} d\bar{z}\bar{r}d\bar{r}d\Psi}{2\pi} = \frac{1}{2}\left[K(1) + \bar{u}_{\xi_o}\right] \qquad (38)$$

For convenience in the following development $\int dvol$ will be taken to mean

$$\int_0^1\int_0^1\int_0^{2\pi} \frac{\bar{r}d\bar{r}d\bar{z}d\Psi}{2\pi}$$

Since the flowfield associated with the uniform boundary sheet is known, and the strength—and hence the velocity field—of the remaining vortex sheets of the wake need only be determined for a single value of $\bar{w}$, it is possible to calculate the thrust coefficient in terms of the solution for $\bar{w} = 0$.

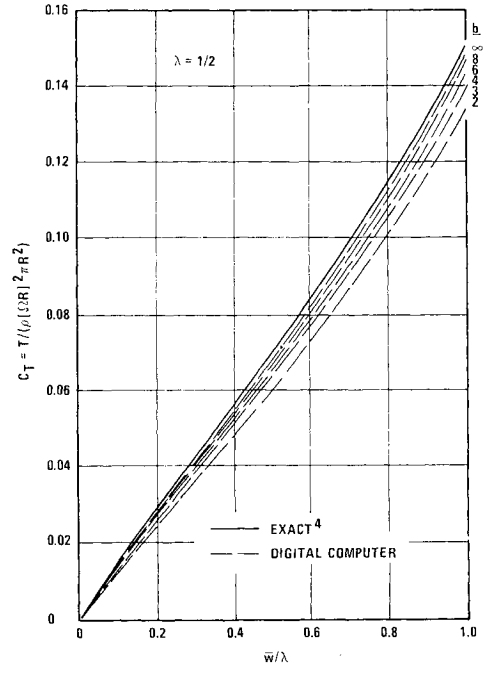

Fig. 5 Variation of thrust coefficient with loading parameter.

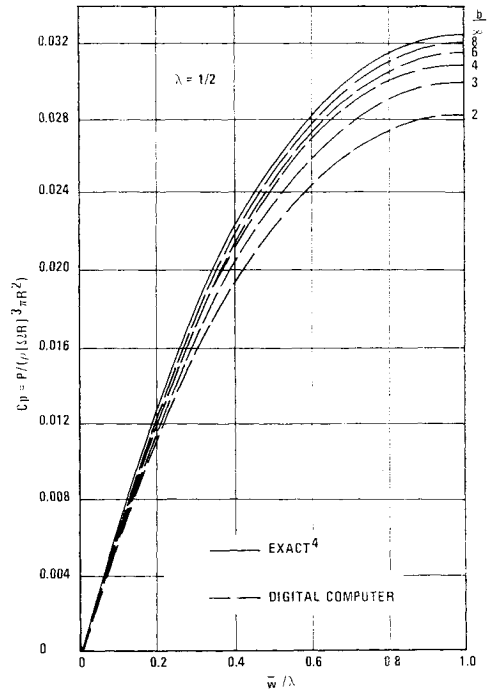

Fig. 6 Variation of induced power coefficient with loading parameter.

The integral terms of eq. (34) can be simplified as follows. The velocities, for $\bar{w} = 0$, associated with the sheets of varying strength (the inner helical sheets and the nonuniform boundary sheets) are denoted by the subscript *vs*. The velocities associated with the uniform boundary sheet are known so that the disturbance velocities can be written as

$$\bar{u}_z = G\bar{u}_{z_{vs}} + \{1 - [G\lambda^2/(1+\lambda^2)]\},\ \bar{u}_\psi = G\bar{u}_{\psi_{vs}},\ \bar{u}_r = G\bar{u}_{r_{vs}}$$

The $\bar{u}_z^2$ term of the C_T equation can be written as

$$\int \bar{u}_z^2 dvol = G^2 \int \bar{u}_{z_{vs}} dvol + 2G\left(1 - \frac{G\lambda^2}{1+\lambda^2}\right) \int \bar{u}_{z_{vs}} dvol + \frac{1}{2}\left(1 - \frac{G\lambda^2}{1+\lambda^2}\right)^2$$

The remaining terms become

$$\int \bar{u}_\Psi^2 dvol = G^2 \int \bar{u}_{\Psi_{vs}}^2 dvol,\ \int \bar{u}_r^2 dvol = G^2 \int \bar{u}_{r_{vs}}^2 dvol$$

$$\int \bar{u}_{z_R}^2 dvol = G^2 \int \bar{u}_{z_{R_{vs}}}^2 dvol + 2G\left(1 - \frac{G\lambda^2}{1+\lambda^2}\right) \times \int \bar{u}_{z_{R_{vs}}} dvol + \frac{1}{2}\left(1 - \frac{G\lambda^2}{1+\lambda^2}\right)^2$$

$$\int \bar{u}_{\Psi_R}^2\, dvol = G^2 \int \bar{u}_{\Psi R_{vs}}^2\, dvol$$

Further, from Eq. (37) and Eq. (38)

$$\int \bar{u}_{z_R}\, dvol = \tfrac{1}{2}\left(GK_0(1) + 1 - G\right) \text{ and } \int \bar{u}_z|_{\bar{w}=0}\, dvol = \tfrac{1}{2}\kappa_0$$

where $K_0(1)$ and κ_0 are the values for $\bar{w} = 0$.

Then

$$\frac{1}{2}\kappa_0 = \int \bar{u}_{z_{vs}}\, dvol + \frac{1}{2}\left(\frac{1}{1+\lambda^2}\right) \text{or}$$

$$\int \bar{u}_{z_{vs}}\, dvol = \frac{1}{2}\left(\kappa_0 - \frac{1}{1+\lambda^2}\right)$$

Substituting these results into Eq. (34) and defining

$$\epsilon_0 = \int_0^1\int_0^1\int_0^{2\pi}\left[\bar{u}_{z_{vs}}{}^2 - \bar{u}_{r_{vs}}{}^2 - \bar{u}_{\Psi_{vs}}{}^2 + \bar{u}_{z_{R_{vs}}}{}^2 + \bar{u}_{\Psi_{R_{vs}}}{}^2\right]\frac{\bar{r}d\bar{r}d\bar{z}d\Psi}{2\pi} \quad (39)$$

yields

$$C_T = \bar{w}^2\left[G\left(\frac{\lambda}{\bar{w}} + 1 - \frac{G\lambda^2}{1+\lambda^2}\right)\kappa_0 - \frac{G^2\lambda^2}{1+\lambda^2}K_0(1) + G^2\epsilon_0 + \left(1-G\right)\left(\frac{\lambda}{\bar{w}} + 1 - 2\frac{G\lambda^2}{1+\lambda^2}\right) - \left(1 - \frac{G\lambda^2}{1+\lambda^2}\right)^2\right] \quad (40)$$

where ϵ_0 must be numerically integrated from the results of the $\bar{w} = 0$ solution.

The ideal power required by the heavily loaded ducted fan can be calculated through a consideration of the induced energy loss in the wake. Following Theodorsen,[3] the energy loss is given by the methods of classical mechanics as

$$Q\Omega - TV_\infty = E = \frac{b\Omega}{2\pi(V_\infty + w)}\int\left[\frac{1}{2}\rho V_\infty v^2 + u_z\left(\frac{1}{2}\rho v^2 + p - p_\infty\right)\right]dvol$$

where Q is the torque and $v^2 = u_z{}^2 + u_r{}^2 + u_\Psi{}^2$. From Eq. (32) $p_\infty - p = \frac{1}{2}\rho(V^2 - V_R{}^2) - \rho(V_\infty + w)(u_z - u_{z_R})$ so that

$$E = b\Omega\rho/2\pi(V_\infty + w) \times \int[\tfrac{1}{2}v^2V_\infty + wu_z{}^2 + u_z(\tfrac{1}{2}V_R{}^2 - u_{z_R}w)]\,dvol$$

Then, defining a nondimensional energy loss as $e = E/[\rho(\Omega R)^3\pi R^2]$ yields

$$e = 2\bar{w}^3\int_0^1\int_0^1\int_0^{2\pi}\left[\bar{u}_z{}^2 + \frac{1}{2}\left(\frac{\lambda}{\bar{w}} - 1\right)\bar{v}^2 + \frac{1}{2}\bar{u}_z\bar{v}_R{}^2 - \bar{u}_z\bar{u}_{z_R}\right]\frac{\bar{r}d\bar{r}d\bar{z}d\Psi}{2\pi}$$

Dividing the velocities into those associated with the uniform boundary sheet and those associated with the variable strength sheets, the expression for e can be calculated in terms of G and the $\bar{w} = 0$ solution as was done for the thrust coefficient; e then becomes

$$e = \bar{w}^3\left\{G\left[\frac{\lambda}{\bar{w}} + \frac{1}{2}\left(1 - \frac{G\lambda^2}{1+\lambda^2}\right)\right]\left(1 - \frac{G\lambda^2}{1+\lambda^2}\right)\left(\kappa_0 - \frac{1}{1+\lambda^2}\right) - \frac{G^2\lambda^2}{1+\lambda^2}\left(1 - \frac{G\lambda^2}{1+\lambda^2}\right)\left(K_0(1) - \frac{1}{1+\lambda^2}\right) + \frac{1}{2}\left(\frac{\lambda}{\bar{w}} - 1\right)\left(1 - \frac{G\lambda^2}{1+\lambda^2}\right)^2 + \frac{1}{2}\left(1 - \frac{G\lambda^2}{1+\lambda^2}\right)^3 +$$

$$G^2\left(\frac{\lambda}{\bar{w}} + 1\right)\int \bar{u}_{z_{vs}}{}^2 dvol + G^2\left(\frac{\lambda}{\bar{w}} - 1\right)\int\left(\bar{u}_{\Psi_{vs}}{}^2 + \bar{u}_{r_{vs}}{}^2\right) \times dvol + G^2\left(1 - \frac{G\lambda^2}{1+\lambda^2}\right)\int\left(\bar{u}_z{}^2{}_{vs_R} + \bar{u}_\Psi{}^2{}_{vs_R}\right)dvol - 2G^3\frac{\lambda^2}{1+\lambda^2}\int \bar{u}_{z_{vs}}\,\bar{u}_{z_{vs_R}}\,dvol + G^3\int \bar{u}_{z_{vs}}\left(\bar{u}_z{}^2{}_{vs_R} + \bar{u}_\Psi{}^2{}_{vs_R}\right)dvol\Big\} \quad (41)$$

Of the remaining integral terms the first three are evaluated in the calculation of ϵ_0 for the thrust coefficient; the last two must be numerically integrated in a similar manner for the $\bar{w} = 0$ case. Defining a power coefficient as $C_p = P/[\rho(\Omega R)^3\pi R^2]$ yields

$$C_p = (\lambda - \bar{w})C_T + e \quad (42)$$

The induced efficiency is then given by

$$\eta_i = [(\lambda - \bar{w})C_T]/[(\lambda - \bar{w})C_T + e] \quad (43)$$

Results

The numerical methods required to generate the solutions for $\bar{w} = 0$ were checked against existing experimental and theoretical results in the literature and are discussed in Ref. 2. Some sample results are shown in Fig. 4 to illustrate the effect of the blade number b on the nondimensional blade bound vortex strength distribution. In Figs. 5 and 6 are shown some sample results for thrust and power coefficient variation with $\bar{w}$ for fans with increasing numbers of blades. The exact results by Gray,[4] for the limit case of a heavily loaded ducted fan with an infinite number of blades, are included to illustrate the convergence of the finite bladed system for increasing blade number. From these results the method appears to be satisfactory and work is now proceeding on the generation of tables for C_p, C_T, η_i, and $K_0(x)$ for a broad range of b, λ, and $\bar{w}$.

References

[1] Betz, A., "Screw Propellers with Minimum Energy Loss," Technical Translation 736, 1958, National Research Council of Canada, Ottawa, Canada.

[2] Gray, R. B. and Wright, T., "Determination of the Design Parameters for Optimum Heavily Loaded Ducted Fans," AIAA Paper 69-222, Atlanta, Ga., 1969.

[3] Theodorsen, T., *Theory of Propellers*, McGraw-Hill, New York, 1948.

[4] Gray, R. B., "Analysis of the Heavily Loaded Infinite Bladed Ducted Fan," unpublished.

SYNOPTIC: New Longitudinal Handling Qualities Data—Carrier Approach, George E. Miller, Princeton University, Princeton, N. J.; *Journal of Aircraft*, Vol. 7, No. 5, pp. 519–522.

Aircraft Handling, Stability, and Control

Theme

A flight evaluation of the flying qualities associated with variations in short-period frequency (ω_{sp} range of 0.6–2.0), lift curve slope (L_α/V range of 0.6–1.35), and the use of direct lift control. Navy test pilot evaluations in the form of Cooper-Harper ratings were obtained for a simulated carrier approach task in turbulence with a variable stability aircraft.

Content

Average pilot ratings and the matrix of configurations are shown in Fig. 1. As can be seen, there is very little difference among configurations with respect to the ability of the pilot to perform the carrier landing task. At the good damping ratio of $\zeta_{sp} = 0.75$ of these tests, the difference in pilot rating between the best and poorest configuration was less than one unit.

A comparison of the data of Fig. 1 with that obtained in similar studies is shown in Fig. 2. The data of Eney and Mooij were both obtained at Princeton using the same variable stability aircraft, Navy carrier qualified pilots, and task as the data of this paper (Miller). The data of Cornell are also flight data, obtained with a variable stability T-33 on a landing approach task. There is agreement among the data obtained in flight; however, a difference exists with the recent results obtained with a moving base simulator (Grumman boundary). Although the lower short-period frequency (ω_{sp}) and minimum g response ($n_{z\alpha}$) boundaries appear reasonable based on flight data, there is a large discrepancy regarding high short-period frequency at low values of $n_{z\alpha}$. A possible explanation is the constraint of constant stick force per $g(F_s/g = 12$ lb/$g)$ of the moving base simulator tests (F_s/g of the flight data is shown in Fig. 2). This could result in an overly sensitive control response at the higher short-period frequencies.

The pilots also evaluated a proportional direct lift control via a separate thumbwheel controller on top of the control stick. Maximum authority was limited to ± 0.15 g. Pilots readily adapted to using this control and found that altitude control close to touchdown was improved with its use.

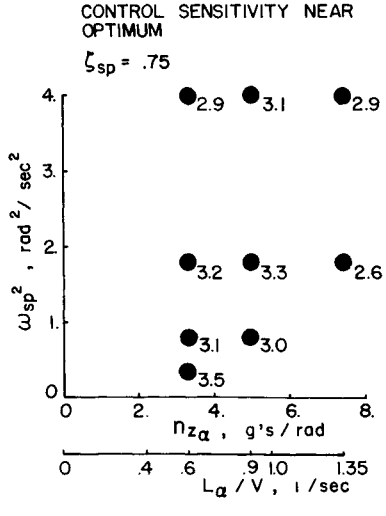

Fig. 1 Pilot ratings of longitudinal short-period characteristics.

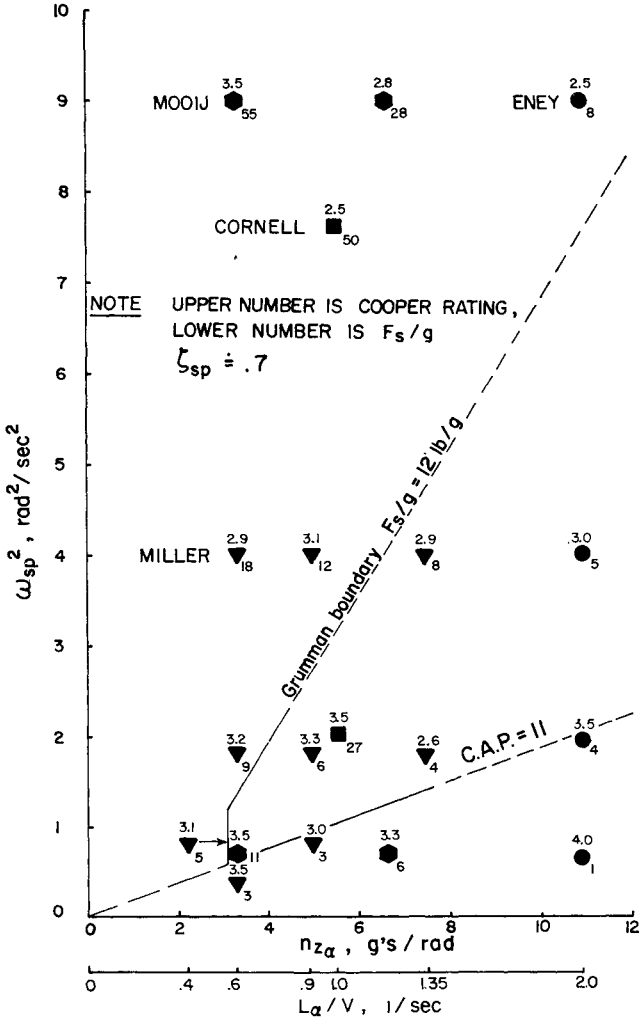

Fig. 2 Pilot rating and stick force/g data comparison.